

Precision and accuracy of R_2 and R_2^* estimation with spin- and gradient-echo EPI

Heiko Schmiedeskamp¹, Matus Straka¹, Thomas Christen¹, Greg Zaharchuk¹, and Roland Bammer¹
¹Department of Radiology, Stanford University, Stanford, CA, United States

INTRODUCTION – Combined spin-echo (SE) and gradient-echo (GE) EPI acquisitions are beneficial for quantitative PWI and facilitate the separation of microvascular and large vessel signals [1], which found application in tumor imaging [2]. With such a pulse sequence, R_2 and R_2^* mapping with a temporal resolution of less than 2 seconds is possible, and it can be used for vessel-size imaging (VSI) [3] and the determination of tissue oxygen extraction fraction [4]. High accuracy in the estimation of R_2 and R_2^* is important for the proper determination of these parameters. For DSC-PWI and dynamic approaches in VSI, it is crucial to obtain R_2 and R_2^* estimates with high temporal stability (precision).

To determine simultaneous estimates of R_2 and R_2^* , a spin- and gradient-echo (SAGE) EPI pulse sequence has recently been introduced [5]. SAGE EPI data can be processed based on Eq. 1, to obtain T_1 -independent estimates of R_2 and R_2^* [6]. With combined spin- and gradient-echo measurements, slice profile differences between excitation and refocusing pulse are challenging, leading to different signal magnitudes before (S_0^I) and after (S_0^{II}) the refocusing pulse. The objective of this study was to analyze the precision and accuracy of R_2 and R_2^* estimates in dynamic studies without slice profile correction and with two different methods to correct for non-matching slice profiles.

THEORY – In Eq. 1, $S^I(t)$ and $S^{II}(t)$ denote the signals before and after the spin-echo refocusing pulse. With a correction term $\delta = S_0^I/S_0^{II}$ and joint estimation of R_2 & R_2^* using Eq. 1, estimation errors of R_2 & R_2^* are greatly reduced compared to an approach assuming matching slice profiles [6].

$$S^I(t) = S_0^I \cdot e^{-t \cdot R_2^*} \quad 0 < t < TE/2 \quad (1)$$

$$S^{II}(t) = S_0^{II} \cdot e^{-TE \cdot (R_2^* - R_2)} \cdot e^{-t \cdot (2 \cdot R_2 - R_2^*)} = \frac{S_0^I}{\delta} \cdot e^{-TE \cdot (R_2^* - R_2)} \cdot e^{-t \cdot (2 \cdot R_2 - R_2^*)} \quad TE/2 < t \leq TE$$

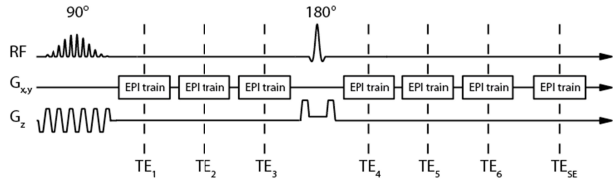


Fig. 1: SAGE EPI pulse sequence diagram.

METHODS – Image acquisition was performed at 1.5 T using the SAGE EPI pulse sequence shown in Fig. 1. Measurements were acquired with a parallel imaging acceleration factor of $R = 3$, and they were repeated 69 times with $TR = 1800$ ms and $TE_{SAGE,1-7} = 12.0, 23.9, 35.9, 59.6, 71.6, 83.5, 100.0$ ms. To determine the precision of R_2 and R_2^* estimates, all 7 echo trains were used for parameter estimation. Specifically, three different methods were assessed:

- 1) 3-parameter estimation (S_0, R_2, R_2^*), assuming matching slice profiles, i.e. $S_0^I = S_0^{II}$,
- 2) 4-parameter estimation ($S_0^I, S_0^{II}, R_2, R_2^*$), assuming non-matching slice profiles, i.e. $S_0^I = \delta \cdot S_0^{II}$,
- 3) 3-parameter estimation with predetermined δ ; here, δ was derived using 4-parameter estimation from the voxel-wise signal average during a pre-defined baseline period of 10 time points, equivalent to the pre-bolus period in a typical DSC-PWI experiment. Subsequently, for each time point, Eq. 1 was solved for 3 parameters.

For each processing method, voxel-wise standard deviations of R_2 (σ_{R_2}) and R_2^* ($\sigma_{R_2^*}$) were measured over all time points to assess the precision of R_2 and R_2^* estimates, a metric for signal stability in DSC-PWI. In addition, the accuracy of R_2 and R_2^* estimates was determined through comparisons with reference data obtained in 7 SE EPI measurements with varying $TE_{SE,1-7} = 35-95$ ms and a 7-echo GE EPI acquisition with $TE_{GE,1-7} = 11.6-83.0$ ms.

RESULTS – Fig. 2 shows the precision and accuracy of R_2 estimates in a human experiment. The precision of estimated R_2 was considerably larger using 4-parameter estimation (average $\sigma_{R_2} = 1.01$ s⁻¹), compared to 3-parameter estimation ignoring δ ($\sigma_{R_2} = 0.42$ s⁻¹). If δ was estimated based on 10 baseline scans and then used as a predetermined parameter in the 3-parameter estimation model, $\sigma_{R_2} = 0.42$ s⁻¹ resulted. Thus, the precision of R_2 estimates using method 3 was as good as with method 1. The precision of R_2^* was nearly identical with all three methods ($\sigma_{R_2^*} = 1.32$ s⁻¹, 1.27 s⁻¹, and 1.32 s⁻¹). Despite high precision in the estimation of R_2 and R_2^* , however, large overestimations of R_2 (+63.8%) and R_2^* (+78.1%) occurred if slice profile mismatches were ignored (method 1). R_2 and R_2^* estimates in the other two approaches were more accurate: average R_2 (R_2^*) was 1.0% (0.4%) larger than the reference value with method 2, and 0.3% larger (0.4% smaller) with method 3 (cf. Fig. 2).

Fig. 2: Precision & accuracy of R_2 estimates with SAGE EPI.

and R_2^* (+78.1%) occurred if slice profile mismatches were ignored (method 1). R_2 and R_2^* estimates in the other two approaches were more accurate: average R_2 (R_2^*) was 1.0% (0.4%) larger than the reference value with method 2, and 0.3% larger (0.4% smaller) with method 3 (cf. Fig. 2).

DISCUSSION – The analysis of precision of R_2 and R_2^* showed that the 4-parameter estimation led to a considerable increase in temporal fluctuations of R_2 when compared to R_2 estimates determined from 3-parameter estimation methods. As shown here, the effective slice profile mismatch could be determined in a baseline measurement and thereafter applied to the MR signal equation (Eq. 1) as an approximated term. This method revealed precisions of R_2 and R_2^* estimates similar to those achieved without δ -correction, but with the advantage of better accuracy in the estimation of the transversal relaxation parameters. Thus, to achieve high precision and high accuracy, it is recommended to use 3-parameter estimation with a predetermined slice profile correction factor δ , particularly in presence of noisy datasets or large slice profile mismatches.

REFERENCES – [1] Boxerman, et al. MRM 1995;34:555–566, [2] Donahue, et al. MRM 2000;43:845–853, [3] Kiselev, et al. MRM 2005;53:553–563, [4] Christen, et al. Proc. ISMRM 2011, p.2729, [5] Newbould, et al. Proc. ISMRM 2007 p.1451, [6] Schmiedeskamp, et al. MRM 2011;doi:10.1002.

ACKNOWLEDGEMENTS – NIH (5R01EB002711, 5R01EB008706, 5R01EB006526, 5R21EB006860, 2P41RR009784), Lucas Foundation, Oak Foundation.